Monte Carlo method for the simulation of electronic noise in semiconductors

Tilmann Kuhn,* Lino Reggiani, and Luca Varani

Dipartimento di Fisica dell'Universita degli Studi di Modena e Centro Interuniversitario di Struttura della Materia del Ministero della Pubblica Istruzione, via Campi 213/A, I-41100 Modena, Italy

Vladimir Mitin

Institute of Semiconductors, Academy of Sciences of the Ukrainian S.S.R., Kiev, U.S.S.R.

We present a general theory to investigate the electronic noise in the presence of scattering as well as of generation-recombination processes. An exact decomposition procedure of the current spectral density is given that, in addition to fluctuations in carrier velocity and number, shows the presence of a cross term coupling both fluctuations. Four correlation functions are thus found to be needed to evaluate all terms. To this purpose, the Monte Carlo method is shown to provide a unifying microscopic calculation of these functions. We consider the case of p-type Si at 77 K with a generation-recombination mechanism given by the capture at shallow impurities assisted by acoustic phonons. Then, the theoretical results are compared with existing mesoscopic theories as well as with available experimental results.

I. INTRODUCTION

The Monte Carlo (MC) method, by providing a microscopic simulation of the dynamics of an ensemble of particles in a given physical system,[1] offers a unique theoretical approach for investigating the different sources of noise and the corresponding spectral densities. In particular, since by construction it is equivalent to the solution of the appropriate master equation for any strength of the applied electric field, it applies to Ohmic as well as to non-Ohmic (hot-carrier) conditions.

Different authors in recent years have applied this method to several physical conditions.[2−7] In particular, previous efforts of Reggiani and collaborators at Modena have succeeded in interpreting noise data in Si with and without carrier-carrier scattering[8,9] and in the presence of generation-recombination (GR) phenomena.[10−12]

In this paper we review and extend[13,14] the general theory underlying the application of the MC method to the simulation of electronic noise in homogeneous semiconductors. By allowing for GR processes within a two-level model, we provide an exact decomposition procedure for the current spectral density which, in addition to fluctuations in carrier velocity and number, shows the presence of a cross-correlation contribution due to the coupling between these fluctuations. In this way, we offer a unifying microscopic interpretation of electronic noise which is given at a kinetic level. In particular, for the case of number fluctuations, this approach overcomes previous mesoscopic theories based on relaxation-time approaches.[15−17] By considering capture processes at shallow centers assisted by acoustic phonons as a typical source of GR noise, the theoretical analysis is applied to the case of p-type Si at 77 K where a comparison with existing analytical results and available experiments is carried out.

The paper is organized as follows. Section II presents the theoretical approach at the basis of an exact decomposition procedure of the current spectral density. In Sec. III we apply the general theory to the simplified case of noninteracting particles. The details of the MC simulation are given in Sec. IV where the calculations performed for the case of p-type Si at 77 K are reported and the comparison with available experiments is given. The main conclusions are drawn in Sec. V. Three appendixes complement the theoretical calculations.

II. THEORY

We consider the following physical model. (i) Two terminal nondegenerate semiconductor device of length L and cross-sectional area A. (ii) Strongly extrinsic regime (i.e., negligible compensation) with a two-level conduction mechanism, the impurity centers, and the conducting band. (iii) Stationary and space homogeneous conditions.

Let us recall the definition of the current spectral density at frequency f, $S_I(f)$, given by[18]

$$S_I(f) = 2 \int_{-\infty}^{\infty} \exp(i2\pi f t) \langle \delta I(0) \delta I(t) \rangle dt , \tag{1}$$

where $\delta I(t) = I(t) - \langle I \rangle$ is the current fluctuation around the average value $\langle I \rangle$, and the angular brackets denote an ensemble average which, by assuming ergodicity, can be performed as time average.

The total current $I(t)$, as measured in the outside circuit, can be expressed in the following two equivalent forms[19] (see Appendix A):

$$I(t) = \frac{e}{L} N(t) v_d(t) = \frac{e}{L} N_I v_d^r(t) , \tag{2}$$

where e is the absolute value of the electron charge, $N(t)$

is the instantaneous number of free carriers, $v_d(t)$ is the instantaneous value of the free-carrier drift velocity (which neglects the trapping time but accounts for the change in velocity between the trapping and detrapping instants), N_I is the total number of carriers which, for negligible compensation, is equal to the number of impurity centers inside the device, and $v_d^r(t)$ is the instantaneous value of the reduced drift velocity of the total number of carriers (which accounts for the time spent by the carriers on the impurities, the so-called trapping time).

The instantaneous quantities in Eq. (2) are defined as follows:

$$N(t)=\sum_{i=1}^{N_I} u_i(t)=N_I u(t) , \qquad (3)$$

where $u_i(t)$ is the random telegraph signal: $u_i(t)=1$ when the particle is free and $u_i(t)=0$ when the particle is trapped, and $u(t)$ is the instantaneous value of the fraction of free carriers:

$$v_d(t)=\frac{1}{N(t)}\sum_{i=1}^{N(t)} v_i(t) , \qquad (4)$$

where $v_i(t)$ is the instantaneous value of the free-carrier velocity component in the field direction of the particle i:

$$v_d^r(t)=\frac{1}{N_I}\sum_{i=1}^{N_I} v_i^r(t) , \qquad (5)$$

where $v_i^r(t)$ is the instantaneous value of the reduced velocity component in the field direction of the particle i: $v_i^r(t)=v_i(t)$ when the particle is in the conducting band and $v_i^r(t)=0$ when the particle is trapped.

From the above definitions we notice the following property:

$$v_d^r(t)=\frac{N(t)}{N_I}v_d(t)=u(t)v_d(t) . \qquad (6)$$

Thus, the instantaneous current fluctuation in the outside circuit, $\delta I(t)$, is given by the two equivalent forms (see Appendix B):

$$\delta I(t)=\frac{e}{L}N_I \delta v_d^r(t)\simeq \frac{e}{L}[\langle N\rangle\delta v_d(t)+\langle v_d\rangle\delta N(t)] , \qquad (7)$$

where $\delta v_d^r(t)=v_d^r(t)-\langle v_d^r\rangle$, $\delta v_d(t)=v_d(t)-\langle v_d\rangle$, $\delta N(t)=N(t)-\langle N\rangle$, and the right-hand side (RHS) of Eq. (7) follows from linearization of the RHS of Eq. (2). We notice that the use of the reduced velocity has the remarkable advantage of describing the current fluctuations in terms of a single fluctuating quantity.

The last expression on the right-hand side of Eq. (7) lends itself to an exact decomposition of $S_I(f)$ in terms of different noise sources. Indeed, from Eqs. (1) and (7), $S_I(f)$ can be expressed in the following two equivalent forms:[13]

$$S_I(f)=\frac{2e^2}{L^2}N_I^2 \int_{-\infty}^{\infty} \exp(i2\pi ft)\langle \delta v_d^r(0)\delta v_d^r(t)\rangle dt , \qquad (8a)$$

$$S_I(f)=S_{Iv_d}(f)+S_{Igr}(f)+S_{Icr}(f) , \qquad (8b)$$

where

$$S_{Iv_d}(f)=\frac{2e^2}{L^2}\langle N\rangle^2 \int_{-\infty}^{\infty} \exp(i2\pi ft)\langle \delta v_d(0)\delta v_d(t)\rangle dt , \qquad (9)$$

$$S_{Igr}(f)=\frac{2e^2}{L^2}\langle v_d\rangle^2 \int_{-\infty}^{\infty} \exp(i2\pi ft)\langle \delta N(0)\delta N(t)\rangle dt , \qquad (10)$$

$$S_{Icr}(f)=\frac{2e^2}{L^2}\langle N\rangle\langle v_d\rangle$$
$$\times \int_{-\infty}^{\infty} \exp(i2\pi ft)[\langle \delta N(0)\delta v_d(t)\rangle$$
$$+\langle \delta v_d(0)\delta N(t)\rangle]dt . \qquad (11)$$

As seen from Eq. (8b), the total spectral density is decomposed into the sum of three terms which are related to fluctuations in free-carrier velocity (S_{Iv_d}), number (S_{Igr}), and correlation between number and velocity (S_{Icr}), respectively. From their definition in terms of correlation functions [see Eqs. (10) and (11)] it appears that S_{Igr} and S_{Icr} are proportional to $\langle v_d\rangle^2$ and at least to $\langle v_d\rangle$, respectively. Therefore, they describe excess noise and, as expected, vanish at equilibrium and/or when the noise is evaluated perpendicular to the field direction, where $\langle v_d\rangle$ is equal to zero. Of course, S_{Igr} and S_{Icr} are zero when the traps are fully ionized, since it implies that at any time $\delta N(t)=0$.

By linearizing Eq. (6) as

$$\delta v_d(t)=\frac{\delta v_d^r(t)}{\langle u\rangle}-\frac{\langle v_d^r\rangle}{\langle u\rangle^2}\delta u(t) , \qquad (12)$$

the three correlation functions in the RHS of Eqs. (9) and (11) can be conveniently expressed in terms of the reduced velocity fluctuations as

$$\langle \delta v_d(0)\delta v_d(t)\rangle=\frac{1}{\langle u\rangle^2}\langle \delta v_d^r(0)\delta v_d^r(t)\rangle$$
$$+\frac{\langle v_d^r\rangle^2}{\langle u\rangle^4}\langle \delta u(0)\delta u(t)\rangle$$
$$-\frac{\langle v_d^r\rangle}{\langle u\rangle^3}[\langle \delta v_d^r(0)\delta u(t)\rangle$$
$$+\langle \delta u(0)\delta v_d^r(t)\rangle] , \qquad (13)$$

$$\langle \delta N(0)\delta v_d(t)\rangle=\frac{N_I}{\langle u\rangle}\langle \delta u(0)\delta v_d^r(t)\rangle$$
$$-\frac{\langle v_d^r\rangle N_I}{\langle u\rangle^2}\langle \delta u(0)\delta u(t)\rangle , \qquad (14)$$

$$\langle \delta v_d(0)\delta N(t)\rangle=\frac{N_I}{\langle u\rangle}\langle \delta v_d^r(0)\delta u(t)\rangle$$
$$-\frac{\langle v_d^r\rangle N_I}{\langle u\rangle^2}\langle \delta u(0)\delta u(t)\rangle . \qquad (15)$$

Therefore, the knowledge of the four correlation functions in the RHS of Eq. (13) [which are given in terms of $u(t)$ and $v_d^r(t)$] is equivalent to the knowledge of the four correlation functions in Eqs. (9)–(11) [which are given in

terms of $N(t)$ and $v_d(t)$] and thus sufficient to determine the three terms of Eq. (8b) into which the total spectral density is decomposed. Furthermore, the correlation function $\langle \delta v_d(0)\delta v_d(t)\rangle$ can be independently calculated from a simulation that neglects the trapping time but contains GR processes as velocity randomizing events. We notice that, while the cross-correlation functions in the rhs of Eq. (11) can be directly evaluated only by a many-particle simulation, the use of the reduced velocity fluctuations will enable us to evaluate these functions from a one-particle simulation, provided that particle-particle interaction is neglected. This is the subject of the next section.

III. THE CASE OF NONINTERACTING PARTICLES

The calculation of the total spectral density, and of the three terms into which it can be decomposed [see Eq. (8b)], is considerably simplified for the case of noninteracting particles. (Here, particle-particle interaction does not only mean a direct scattering between two carriers, but also a correlation introduced by the occupancy factor of the impurity levels.) Thus, for a single-particle simulation only a linear recombination can be treated. As a matter of fact, in this case we can take advantage of the representation in terms of the reduced velocity fluctuations seen above and calculate the different correlation functions from a one-particle approach. For this purpose, we make use of the following properties (see Appendix C):

$$\langle \delta v_d^r(0)\delta v_d^r(t)\rangle = \frac{1}{N_I}\langle \delta v_i^r(0)\delta v_i^r(t)\rangle , \tag{16}$$

$$\langle \delta N(0)\delta N(t)\rangle = N_I\langle \delta u_i(0)\delta u_i(t)\rangle , \tag{17}$$

$$\langle \delta N(0)\delta v_d(t)\rangle = \frac{1}{\langle u\rangle}\langle \delta u_i(0)\delta v_i^r(t)\rangle$$
$$-\frac{\langle v_d^r\rangle}{\langle u\rangle^2}\langle \delta u_i(0)\delta u_i(t)\rangle , \tag{18}$$

$$\langle \delta v_d(0)\delta N(t)\rangle = \frac{1}{\langle u\rangle}\langle \delta v_i^r(0)\delta u_i(t)\rangle$$
$$-\frac{\langle v_d^r\rangle}{\langle u\rangle^2}\langle \delta u_i(0)\delta u_i(t)\rangle , \tag{19}$$

where $\delta v_i^r(t) = v_i^r(t)-\langle v_d^r\rangle$ and $\delta u_i(t) = u_i(t)-\langle u\rangle$.

As a consequence of Eqs. (16)–(19), Eq. (13) becomes

$$\langle \delta v_d(0)\delta v_d(t)\rangle = \frac{1}{N_I\langle u\rangle^2}\langle \delta v_i^r(0)\delta v_i^r(t)\rangle$$
$$+\frac{\langle v_d^r\rangle^2}{N_I\langle u\rangle^4}\langle \delta u_i(0)\delta u_i(t)\rangle$$
$$-\frac{\langle v_d^r\rangle}{N_I\langle u\rangle^3}[\langle \delta v_i^r(0)\delta u_i(t)\rangle$$
$$+\langle \delta u_i(0)\delta v_i^r(t)\rangle] . \tag{20}$$

The initial values of the correlation functions in Eqs. (17)–(19), in this case of noninteracting particles, can be exactly calculated by noticing that by construction it is

$\langle u_i^2\rangle = \langle u\rangle$ and $\langle u_i v_i^r\rangle = \langle v_d^r\rangle$. Therefore, we obtain

$$\langle [\delta N(0)]^2\rangle = N_I\langle u\rangle(1-\langle u\rangle) , \tag{20a}$$

$$\langle \delta N(0)\delta v_d(0)\rangle = \langle \delta v_d(0)\delta N(0)\rangle = 0 . \tag{20b}$$

Equation (20b) states that the fluctuations of particle number and drift velocity at equal times are uncorrelated. This is due to the fact that, for independent particles, all scattering and recombination mechanisms depend only on the average numbers of carriers and not on its actual value.

Phenomenological models exist for some autocorrelation functions,[15–17] while very little is known on the cross-correlation functions.[13,14,20] For the case of velocity fluctuations, within a relaxation-time approximation[21] it is

$$\langle \delta v_d(0)\delta v_d(t)\rangle = \langle [\delta v_d(0)]^2\rangle \exp(-t/\tau_c) , \tag{21}$$

where τ_c is an average scattering time related to the mobility, μ, as

$$\mu = \frac{e}{m}\tau_c \tag{21a}$$

(m being the carrier effective mass) and, within an electron temperature model, it is

$$\langle [\delta v_d(0)]^2\rangle = \frac{1}{\langle u\rangle N_I}\frac{k_B T_e}{m} , \tag{21b}$$

k_B being the Boltzmann constant and T_e the electron temperature related to the average energy of the carrier ensemble $\langle \varepsilon\rangle = \frac{3}{2}k_B T_e$.

For the case of number fluctuations, within a relaxation-time approximation, it is[17]

$$\langle \delta N(0)\delta N(t)\rangle = \langle [\delta N(0)]^2\rangle \exp(-t/\tau_l) , \tag{22}$$

where $\langle [\delta N(0)]^2\rangle$ is given by Eq. (20a) and τ_l is the lifetime. For GR processes governed by linear kinetics, it is[17,18]

$$\tau_g = \frac{1}{\gamma} , \tag{22a}$$

$$\tau_r = \frac{\langle u\rangle}{\gamma(1-\langle u\rangle)} , \tag{22b}$$

$$\tau_l = \left[\frac{1}{\tau_g}+\frac{1}{\tau_r}\right]^{-1} = \frac{\langle u\rangle}{\gamma} , \tag{22c}$$

where γ is the generation rate, τ_g the generation time, and τ_r the average (over the energy distribution function) recombination time. We remark that within the approach considered (i.e., relaxation time and linear GR processes), Eqs. (22) are of universal form in the sense

that they are expected to hold independently from the dependence of $\langle u \rangle$ on the intensive variables such as the electric field, temperature, etc. We shall come back to this aspect later.

IV. MONTE CARLO SIMULATION

Calculations are performed for the case of p-type Si, where recent experiments from the Montpellier group are available. To simplify the calculations and make the cpu time accessible, we consider the case of noninteracting particles. The details of the numerical calculation and of the microscopic model are given in Ref. 22, while the parameters entering the simulation are summarized in Table I. If not stated specifically, the Poole-Frenkel effect is neglected. We remark that this microscopic model has been recently used with success to interpret the field-dependent conductivity of lightly doped p-type Si.[23] Therefore, by including GR processes, it generalizes a previous model adequate to describe transport in a conducting band only.[24]

The different correlation functions have been evaluated in the standard way, as for the case of the autocorrelation function of velocity fluctuations (AFVF) in the absence of GR processes.[1] To this end we record the instantaneous values of $u_i(t)$ and $v_i'(t)$ for a sampling time T_0 sufficiently long to detect the vanishing value of the correlation functions (typically $T_0 \simeq 1$ ns) with a mesh of about 10^3 points. Each simulation requires between 2 and 10 h central-processing-unit (CPU) time of a Digital Equipment Corporation VAX 6310 computer. The reason for these long times is the large difference in the time scales involved in the problem: scatterings occur typically on a time scale below 1 ps while the time scale for GR processes is of the order of 100 ps to 1 ns.

The average fraction of ionized carriers is consistently

determined from the ratio between the total time spent in the valence band and the total time of the simulation. Since in the present case by construction it is $\langle u_i^2 \rangle = \langle u \rangle$, Eq. (20a) is exactly verified in MC calculations. Then, both the generation rate and the average recombination rate have been independently determined, respectively, from the ratio between the total time spent in the traps and the total number of generations and from the ratio between the total time spent in the valence band and the total number of recombinations. We have verified that the values of the rates so determined are in good agreement with the expectations of Eqs. (22a) and (22b) for any field strength. On the other hand, the value of the lifetime, as determined by the decay in time of the autocorrelation function of particle-state fluctuations (AFPSF) has been found to be in general not in agreement with the expected value of Eq. (22c), as will be discussed in the following section.

Figure 1 reports the energy dependence of the scattering rates due to the different mechanisms which have been used in the MC calculations.

Figure 2 shows the values of the average energy, the fraction of ionized carriers, and the mobility as a function of the electric field for a typical acceptor concentration. The deviation from unity of different values is known to be due to the onset of hot-carrier conditions.[25,26]

A. Results for the correlation functions

In this section we discuss the time dependence of the reduced correlation functions required for our decomposition procedure. These functions are the direct output of
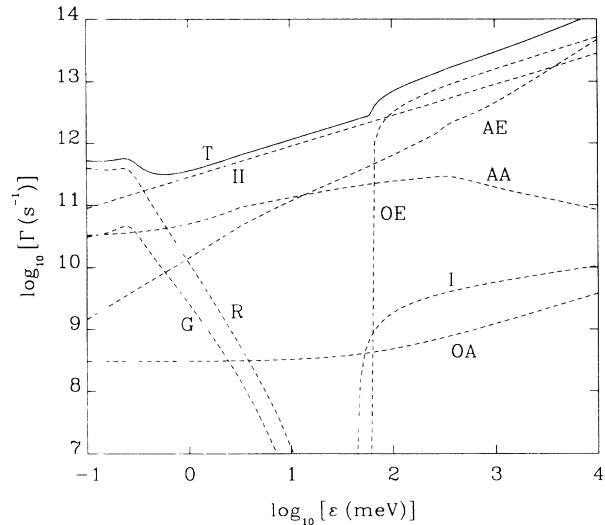
TABLE I. Parameters for p-type Si used in calculations. The effective mass takes into account nonparabolicity and therefore it varies as a function of carrier mean energy between the given values as reported in Ref. 23.

Effective mass	$m_h = (0.53 - 1.26)m_0$
Crystal density	$\rho_0 = 2.32$ g cm^{-3}
Sound velocity	$s = 6.53 \times 10^5$ cm s^{-1}
Optical-phonon temperature	$\theta_{op} = 735$ K
Relative static dielectric constant	$\epsilon_r = 11.7$
Acoustic deformation potential	$E_1^0 = 5$ eV
Optical deformation potential	$D_t K = 6 \times 10^8$ eV cm^{-1}
Equilibrium volume recombination rate	$\rho_{eq} = 4.2 \times 10^{-6}$ cm^3 s^{-1}
Equilibrium generation rate	$\gamma = 2.9 \times 10^9$ s^{-1}
Energy of the acceptor level	$\varepsilon_a = 45$ meV
Cross section for impact ionization	$\sigma_g = 5.02 \times 10^{-14}$ cm^2

FIG. 1. Scattering rates Γ as a function of energy ε for p-type Si at 77 K with $N_A = 3 \times 10^{15}$ cm^{-3}. Symbols have the following meaning: AA (acoustic absorption), AE (acoustic emission), OA (optical absorption), OE (optical emission), II (ionized impurity), G (generation), I (impact ionization), R (recombination), T (total). Notice that the generation rate does not contribute to the total rate and its energy scale refers to the final energy of the hole in the valence band.
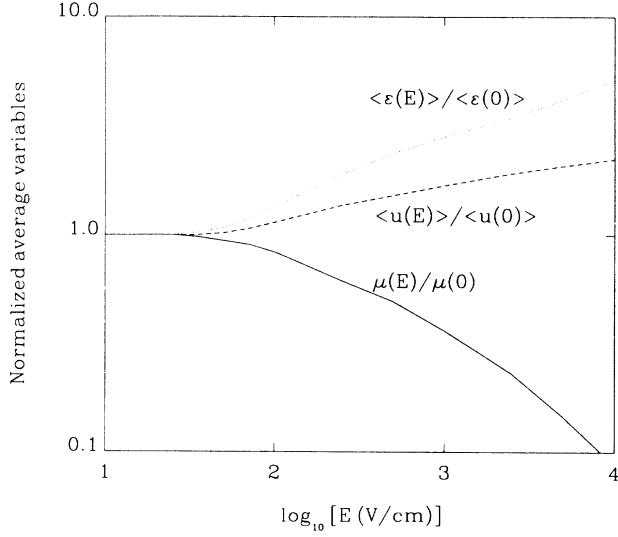
FIG. 2. Average energy, fraction of free carriers, and mobility as a function of the electric field E in p-type Si at 77 K with $N_A = 3 \times 10^{15}$ cm^{-3}. Quantities are normalized to their zero field value.

FIG. 4. The same correlation functions as in Fig. 3 but over a time range of 1500 ps.

the MC simulation. (A complete analysis of the transport phenomenon in terms of a full set of relevant correlation functions involving energy, momentum, and carrier numbers is also possible to be carried out. However, such an analysis, which is of physical interest in itself,[21] is far from the objectives of the present paper and will be presented elsewhere.)

Figure 3 and 4 report the four reduced correlation functions in the RHS of Eq. (20) normalized to their initial time values for an electric field of 50 V/cm (direction
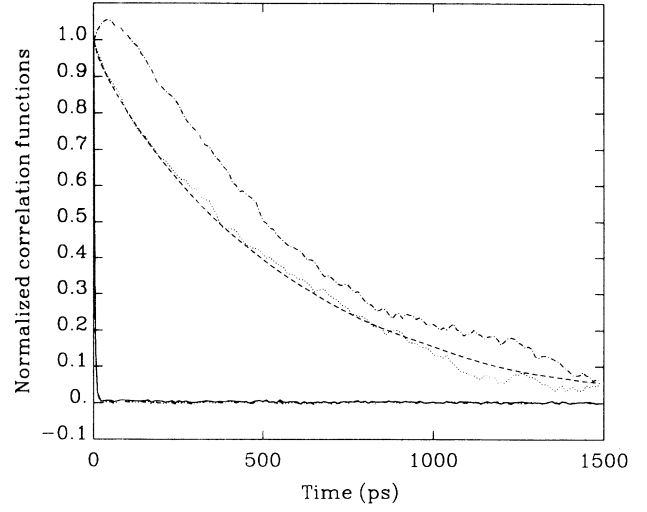
$\langle 100 \rangle$) and an acceptor concentration of 3×10^{15} cm^{-3}. Figure 3 shows the results in the first 15 ps, while Fig. 4 shows the same curves within an extended time range of 1500 ps. (The worse resolution at increasing time of the cross correlations should be ascribed to their small absolute value.) We notice that the autocorrelation function of reduced-velocity fluctuations (AFRVF) decays very fast in the first 10 ps, reflecting the short scattering time associated with the collisions while the carrier is in the conducting band. As a matter of fact, in the whole time range the AFRVF, when appropriately scaled, is found to nearly coincide with the AFVF (now calculated by in-
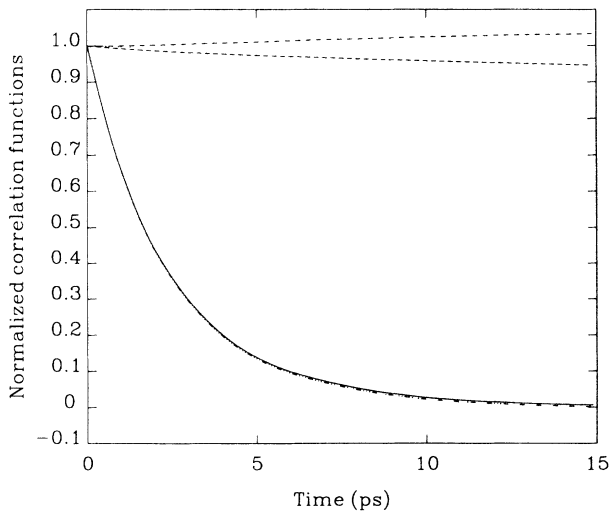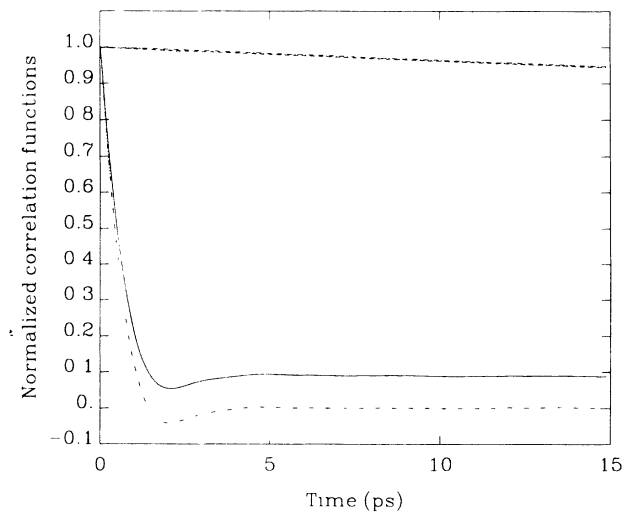

FIG. 3. Correlation functions normalized to their initial value in p-type Si at 77 K with $N_A = 3 \times 10^{15}$ cm^{-3} and an electric field $E = 50$ V/cm over a time range of 15 ps. Solid, dashed, dotted, dot-dashed, and triple-dot-dashed lines refer, respectively, to $\langle \delta v_i^r(0)\delta v_i^r(t) \rangle$, $\langle \delta u_i(0)\delta u_i(t) \rangle$, $\langle \delta u_i(0)\delta v_i^r(t) \rangle$, $\langle \delta v_i^r(0)\delta u_i(t) \rangle$, and $\langle \delta v_d(0)\delta v_d(t) \rangle$.

FIG. 5. Correlation functions normalized to their initial value in p-type Si at 77 K with $N_A = 3 \times 10^{15}$ cm^{-3} and an electric field $E = 2.5$ kV/cm over a time range of 15 ps. Solid, dashed, dotted, dot-dashed, and triple-dot-dashed lines refer, respectively, to $\langle \delta v_i^r(0)\delta v_i^r(t) \rangle$, $\langle \delta u_i(0)\delta u_i(t) \rangle$, $\langle \delta u_i(0)\delta v_i^r(t) \rangle$, $\langle \delta v_i^r(0)\delta u_i(t) \rangle$, and $\langle \delta v_d(0)\delta v_d(t) \rangle$.
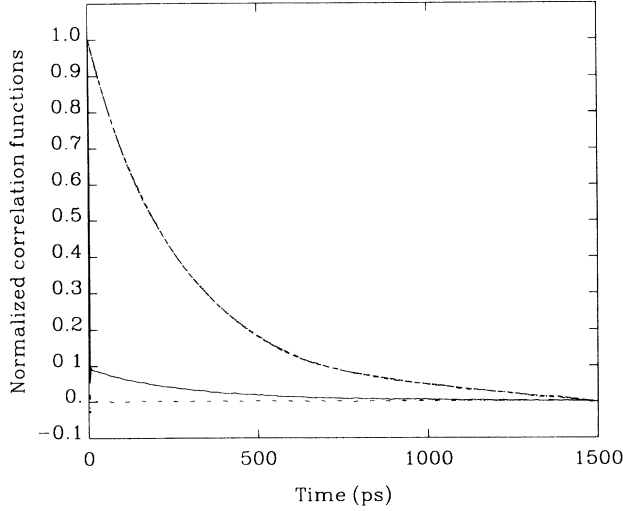
FIG. 6. The same correlation functions as in Fig. 5 but over a time range of 1500 ps.
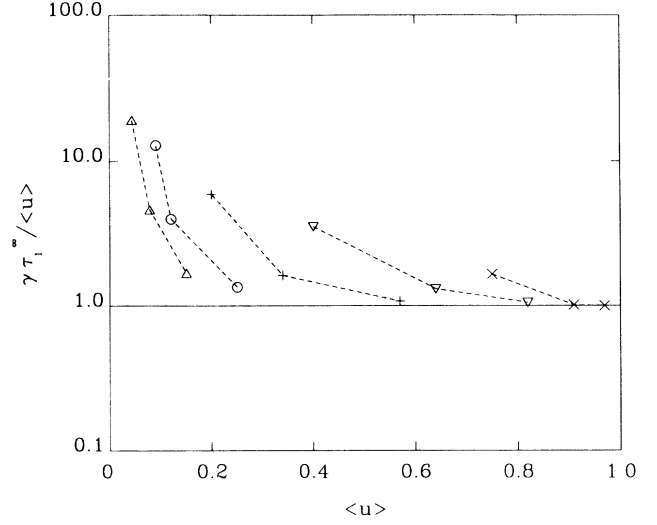

FIG. 7. Values of $\tau_i^\infty \gamma / \langle u \rangle$ as a function of the fraction of free carriers $\langle u \rangle$ in p-type Si at 77 K. Different symbols correspond to the following doping: $\triangle \equiv N_A = 3 \times 10^{17}$ cm^{-3}, $\bigcirc \equiv N_A = 1 \times 10^{17}$ cm^{-3}, $+ \equiv N_A = 1.4 \times 10^{16}$ cm^{-3}, $\nabla \equiv N_A = 3 \times 10^{15}$ cm^{-3}, $\times \equiv N_A = 4 \times 10^{14}$ cm^{-3}. The same symbol refers to MC simulations at electric fields of 0.1, 1, and 10 kV/cm for increasing $\langle u \rangle$, respectively. The solid line refers to the phenomenological approach; the dashed lines are guides to the eyes.

cluding GR processes). However, the AFRVF exhibits a small but very long tail which is responsible for a significant contribution to the spectral density, as will be shown in Sec. IV B. The remaining correlation functions decay slowly in time, reflecting the long lifetime associated with number fluctuations. In particular, we notice that $\langle \delta u_i(0)\delta u_i(t) \rangle$ and $\langle \delta u_i(0)\delta v_i^r(t) \rangle$ exhibit at all times nearly the same dependence within the MC uncertainty, while $\langle \delta v_i^r(0)\delta u_i(t) \rangle$ shows an initial positive slope reaching a maximum before decaying to zero. The former behavior implies that $\langle \delta N(0)\delta v_d(t) \rangle \simeq 0$. The latter behavior implies that $\langle \delta v_d(0)\delta N(t) \rangle$ increases first and then decreases on the time scale of the lifetime. Indeed, if at time $t = 0$ the drift velocity is increased, the carrier energy is also increased. Therefore, a recombination process is less probable (see Fig. 1) and $\delta N(t)$ will increase too. Conversely, if initially the drift velocity is decreased, then the carrier energy is also decreased. Therefore, a recombination process is more probable and $\delta N(t)$ will decrease too. The characteristic time scale for the initial increase of $\langle \delta v_i^r(0)\delta u_i(t) \rangle$ is the energy relaxation time, as verified in MC results. The decay occurs on the time scale of the carrier lifetime, because it is on this time scale that GR processes become independent from each other. From Fig. 1 it can be seen that the recombination rate exhibits a strong decrease above 0.2 meV. Thus, it can be expected that the cross correlations are maximal when $\frac{1}{2}mv_d^2 \simeq 0.2$ meV, which corresponds to electric fields of about 200 V/cm in the present case. This expec-

tation is well verified by MC calculations, as is shown later.

Figures 5 and 6 show the same quantities for a higher electric field of 2.5 kV/cm. With respect to the previous case, we notice that the AFRVF decays faster, reaches a minimum at about 2 ps, increases again, and then exhibits a decay on a long time scale. On the other hand, the time dependence of the remaining reduced correlation functions is found to coincide within the numerical uncertainty. The structure of the AFRVF can be explained as follows: The shortening of the decay time is due to the onset of hot-electron conditions, which, by decreasing the carrier mobility, lead to a shortening of the average scattering time. For the same reason, the coupling between energy and velocity, which is responsible for the negative part of the AFVF seen in the same figure, is the origin of the minimum.[21,27] The long time tail exhibited by all the reduced correlation functions is associated to the carrier lifetime. For completeness, Table II reports the initial values of the correlation functions show in Figs. 3–6 as well as the values of $\langle u \rangle$ and $\langle v_d \rangle$. We remark that all quantities are calculated independently

TABLE II. Initial values of different correlation functions at the given electric field. Calculations refer to the case of p-type Si at 77 K with $N_A = 3 \times 10^{15}$ cm^{-3}.

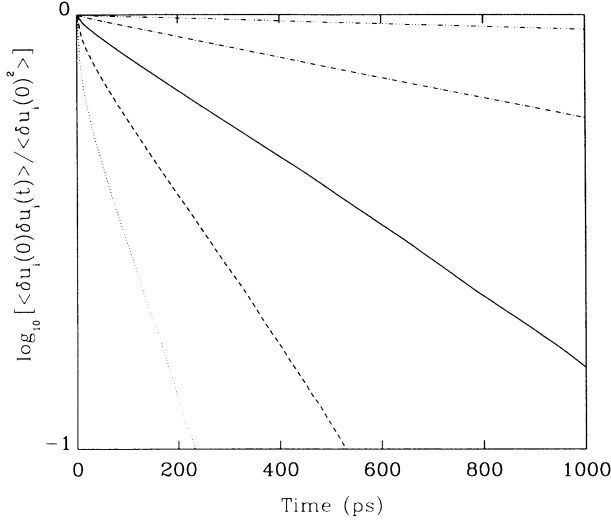| E (V/cm)	$\langle [\delta v_i^r(0)]^2 \rangle$ (10^{13} cm^2/s^2)	$\langle [\delta v_i(0)]^2 \rangle$ (10^{13} cm^2/s^2)	$\langle [\delta u_i(0)]^2 \rangle$	$\langle \delta v_i^r(0)\delta u_i(0) \rangle$ (10^5 cm/s)	$\langle u \rangle$	$\langle v_d \rangle$ (10^6 cm/s)
50	0.77	2.2	0.23	0.91	0.35	0.40
2500	4.7	6.1	0.21	9.6	0.70	4.5

FIG. 8. Autocorrelation function of particle state fluctuations normalized to its equilibrium value in p-type Si at 77 K with $N_A = 3 \times 10^{15}$ cm^{-3} and an electric field $E = 100$ V/cm at different values of the GR rates. Triple-dot-dashed, dash-dotted, solid, dashed, and dotted lines refer to a multiplication of the values ρ_{eq} and γ by a factor of 0.01, 0.1, 1, 10, and 100, respectively.

from the MC simulation and, as a check of consistency, they are found to satisfy rigorously Eqs. (13)–(15), (20a), and (20b).

The determination of the lifetime has been found to be a complicated task. As a matter of fact, a unique definition of a lifetime is problematic since, as a general trend, the AFPSF does not display an exponential decay at the shortest times. There, the decay is generally faster than at longer times, where it really exhibits an exponential tail with a time constant we have called τ_l^∞. Figure 7 compares the universal function (22c), where τ_l^∞ is substituted for τ_l, with the results provided by the MC simulations. We have found significant deviations, the values obtained from the simulation being systematically larger than those predicted by the analytical approach.

To investigate the origin of this nonexponential decay of the AFPSF we have performed a set of simulations by keeping constant all parameters (in particular the ratio ρ_{eq}/γ, ρ_{eq} being the volume recombination rate at equilibrium) but artificially scaling the magnitude of γ and ρ_{eq} over 4 orders of magnitude. In this way, due to the balance equation,[23] the value of $\langle u \rangle$, and thus of

$\langle [\delta u_i(0)]^2 \rangle$, is forced to remain constant while the rate of GR processes scales accordingly to γ and ρ_{eq}. The AFPSF results for $E = 100$ V/cm and $N_A = 3 \times 10^{15}$ cm^{-3} are reported in Fig. 8. The Arrhenius plot evidences an exponential decay in the long time limit and a fast decay of the correlation function at the shortest times, this last becoming more pronounced at increasing values of the GR rates. Table III summarizes the above results, showing that MC results agree well with the analytical theory, with the exception of the lifetime, which, in the long time limit $\langle \tau_l^\infty \rangle$, exhibits values larger than those analytically predicted. In any case, we notice that when lowering the values of the GR rates, the lifetime tends to the expected value.

This anomaly in the behavior of the lifetime is attributed to a nonexponential distribution of the microscopic recombination time, which can be analyzed by plotting the histogram of the number of recombinations associated with a given time interval. Figure 9 reports such a plot at different values of the electric field strength. As can be seen, most recombinations occur at the shortest times and at longer times, within the statistical uncertainty, they exhibit an exponential distribution. By increasing the electric field, this peaking of recombinations at the shortest times, which is found to parallel the behavior of varying the GR rates, is smoothed out. We ascribe these effects to the strong coupling between GR processes and scattering mechanisms, which occurs in the lowest energy region of the carrier energy-distribution function. Indeed, GR processes occur mostly when the carrier energy is below the 1-meV region, where the probability of capture even exceeds that of scattering mechanisms, thus coupling GR and scattering processes at a microscopic level, as seen in Fig. 1. In other words, a carrier after being generated from the trap has a high probability to immediately recombine without having the possibility to visit all the accessible energy regions of the distribution function. Therefore, as pointed out by Price[28] for the similar case of intervalley noise, the carrier can keep memory of the generation process up to the next recombination process in contrast to the case when, once generated, it scatters many times in the conducting band thus losing memory of GR processes. This interpretation is supported by the fact that, at increasing field strengths, MC results get closer to those of the analytical approach at the given field. This is because the onset of hot-carrier phenomena, by decreasing the importance of low-energy processes, tends to reduce the coupling between GR and scattering processes. Of course, this nonexponential de-

TABLE III. Comparison between MC and analytical results for different values of the GR parameters for the quantities reported. Calculatons refer to the case of p-type Si at 77 K with $N_A = 3 \times 10^{15}$ cm^{-3} and $E = 100$ V/cm.

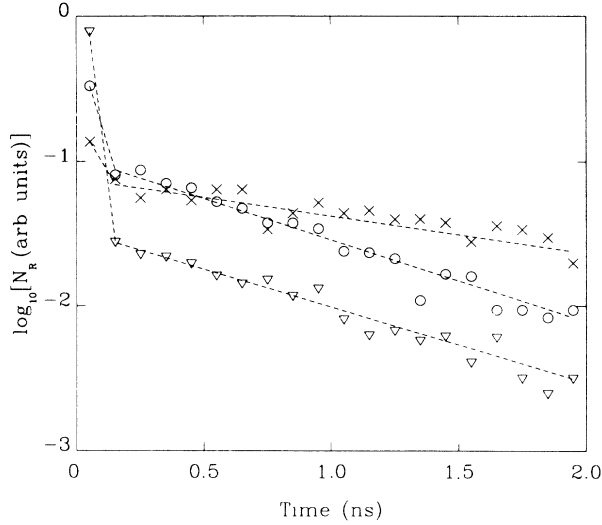|	$10^2 \rho_{eq}, 10^2 \gamma$	$10 \rho_{eq}, 10 \gamma$	ρ_{eq}, γ	$10^{-1} \rho_{eq}, 10^{-1} \gamma$	$10^{-2} \rho_{eq}, 10^{-2} \gamma$	analytical
$\langle u \rangle$	0.37	0.36	0.36	0.37	0.36	0.38
$\langle (\delta u)^2 \rangle$	0.23	0.23	0.23	0.23	0.23	0.24
$\tau_r \gamma$	0.59	0.56	0.58	0.57	0.56	0.61
$\tau_g \gamma$	1.0	0.99	1.0	0.98	1.0	1.0
$\tau_l^\infty \gamma / \langle u \rangle$	94	20	4.4	1.5	1.1	1.0

FIG. 9. Time histogram of the number of recombinations N_R at different values of the electric field in p-type Si at 77 K with $N_A = 3.0 \times 10^{15}$ cm^{-3}. Different symbols correspond to the following fields: $\triangledown \equiv E = 0.1$ kV/cm, $\circ \equiv E = 1$ kV/cm, $\times \equiv E = 10$ kV/cm. The dashed lines are guides to the eyes.

FIG. 11. Current spectral density in the direction of the electric field as a function of frequency f in p-type Si at 77 K for $E = 2.5$ kV/cm with $N_A = 3 \times 10^{15}$ cm^{-3}, $L = 1.5 \times 10^{-2}$ cm and a sample area $A = 3.6 \times 10^{-3}$ cm^2. Solid, dashed, and dotted lines refer to total, velocity, and GR contributions, respectively. Open triangles represent experimental results (Refs. 29 and 30).

cay of the AFPSF becomes more evident at increasing acceptor concentrations, and thus at lowering values of $\langle u \rangle$.

B. Results for the current spectral density

The current spectral density, which is the measurable quantity, is obtained by Fourier transforming the AFRVF, as prescribed by Eq. (8a). Figure 10 reports the numerical results for the low field case shown in Figs. 3
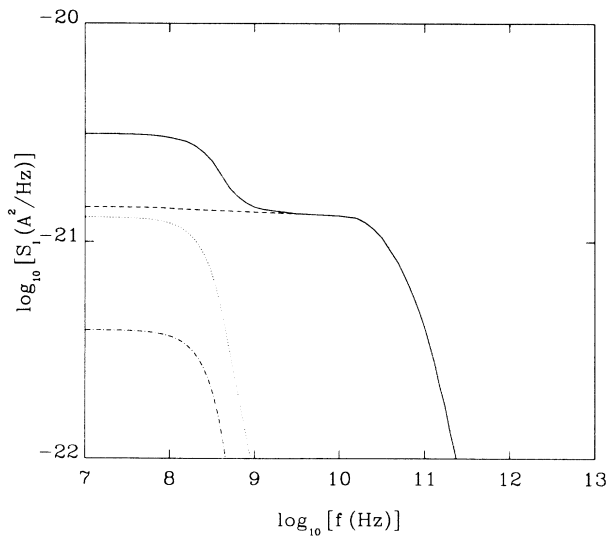
and 4. The total spectral density is decomposed here into three contributions according to Eq. (8b). As can be seen, at low frequencies the GR and velocity contributions are comparable and the cross term, even if of weaker relevance, is easily detectable. Both GR and cross contributions decay with a Lorentzian shape with a corner frequency given by $1/(2\pi\tau_l^\infty)$, while the velocity contribution decays similarly but with a corner frequency given by $1/(2\pi\tau_c)$.

FIG. 10. Current spectral density in the direction of the electric field as a function of frequency f in p-type Si at 77 K for $E = 50$ V/cm with $N_A = 3 \times 10^{15}$ cm^{-3}, $L = 1.5 \times 10^{-2}$ cm, and $A = 3.6 \times 10^{-3}$ cm^2. Solid, dashed, dotted, and dot-dashed lines refer to total, velocity, GR, and cross contributions, respectively, as defined by Eqs. (8)–(11).
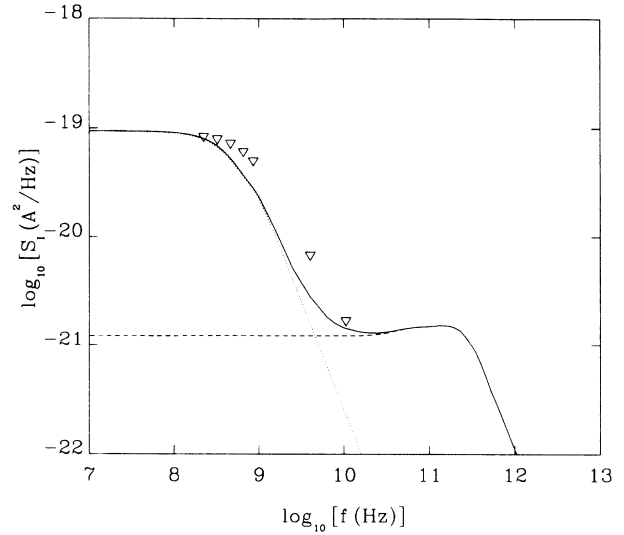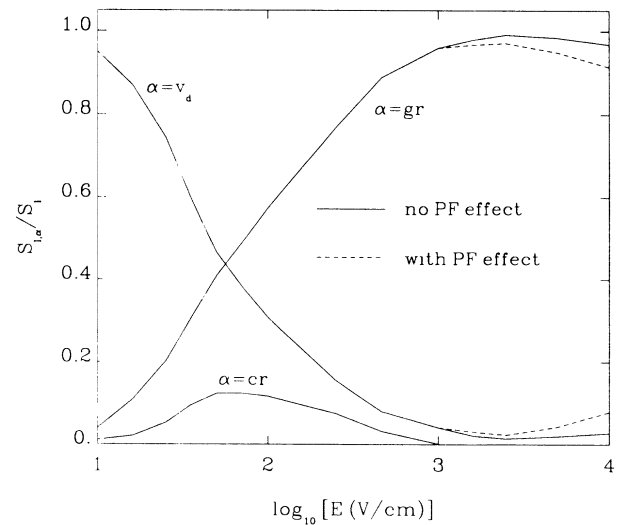

FIG. 12. Relative importance of the different contributions to the low-frequency spectral density as a function of the electric field E for the case of p-type Si at 77 K with $N_A = 3 \times 10^{15}$. The dashed lines refer to the case when the Poole-Frenkel effect is accounted for.

Figure 11 reports the frequency dependence of the spectral densities for the high field case shown in Figs. 5 and 6 as well as recent experimental results.[29,30] Now, at low frequencies the GR contribution is the dominant one while the cross contribution has been found to be of negligible importance and practically not detectable from the simulation. At the highest frequencies only the velocity contribution remains. We notice that this term exhibits a small but detectable increase, before the cutoff, which is associated with the negative part of the AFVF. We remark that the theory satisfactorily agrees with experiments, fully supporting the microscopic model used to treat GR process.

To investigate the role of the cross term, we report in Fig. 12 the relative importance of the different contributions to the low-frequency spectral density as a function of the electric field. At the lowest fields, the velocity con-

tribution is found to dominate in agreement with the Nyquist relationship. In the intermediate region of fields, both GR and cross contributions increase, the former becoming the leading term above 50 V/cm. We notice that the cross term peaks in the region when GR and velocity contributions become comparable and then decreases systematically. In the whole range of fields the cross term remains of smaller importance. These results correct previous overestimations of the cross term[13,14] that have originated from a lack of consistency associated to an independent estimate of the GR contribution alone.

The external field, by modifying the shape of the impurity potential (Poole-Frekel effect), is also responsible for a change of the generation as well as of the volume recombination rate. Accordingly, we have considered a field-dependent generation rate γ_E, based on a three-dimensional Ohmic model,[31,32] given by

$$
\gamma_E = \begin{cases} \gamma \dfrac{4\delta k_B T}{\beta^2 E} \sinh\left[\dfrac{\beta^2 E}{4\delta k_B T}\right] & \text{for } E \le 4\dfrac{\delta^2}{\beta^2} & (23a) \\[4ex] \gamma \dfrac{(k_B T)^2}{\beta^2 E}\left[\exp\left[\dfrac{\delta}{k_B T}\right] + \exp\left[\dfrac{\beta\sqrt{E}-\delta}{k_B T}\right]\left[\dfrac{\beta\sqrt{E}}{k_B T}-1\right] - \dfrac{2\delta}{k_B T}\exp\left[-\dfrac{\beta^2 E}{4\delta k_B T}\right]\right] & \text{for } E > 4\dfrac{\delta^2}{\beta^2}, & (23b) \end{cases}
$$

where $\beta = (e^3/\pi\epsilon_0\epsilon_r)^{1/2}$ is the Poole-Frenkel factor and $\delta = \frac{3}{2}k_B T$ (T is the lattice temperature) is the typical energy, measured from the bottom of the conducting band, for which a bound carrier has a large probability to escape thermally from the impurity level.

The field-dependent volume recombination rate ρ_E, following Ref. 33, has been taken as

$$
\rho_E = \begin{cases} \rho_{eq}\left[1+0.98\dfrac{\beta^2 E}{4\delta k_B T}\right]^{-1} & \text{for } E \le 4\dfrac{\delta^2}{\beta^2} & (24a) \\[3ex] \rho_{eq}\left[1+0.98\dfrac{\beta\sqrt{E}-\delta}{k_B T}\right]^{-1} & \text{for } E > 4\dfrac{\delta^2}{\beta^2}. & (24b) \end{cases}
$$

The calculations which include the Poole-Frenkel effect are reported in Fig. 12 where it is shown that it becomes significant above 3×10^3 V/cm. In the present case, this effect concurs with carrier heating to a further increase of the fraction of free carriers.

Finally, we wish to remark that the model of a linear recombination kinetics, as we have used here, instead of a more appropriate quadratic kinetics, is expected to yield an overestimation of the GR contribution[17] up to a factor 4 in the limit of vanishing values of $\langle u \rangle$. This could require a reconsideration of the values of the GR parameters used here. In any case, to account for a quadratic recombination implies the use of a many-particle simulation with associated CPU times which, for the present model, are not yet accessible.

V. CONCLUSIONS

We have presented a general theory of electronic noise in homogeneous semiconductors that enables an exact decomposition procedure of different noise sources in the presence of generation recombination processes to be carried out. For the case of a two-level model, three contributions are found to determine the current spectral density. These refer to fluctuations in free-carrier velocity, number, and their correlations. To evaluate all contributions, the knowledge of four correlation functions is required. To this purpose, we have shown that the use of the reduced carrier velocity can simplify considerably the calculations, being that it is the only quantity responsible for current fluctuations. In particular, when particle-particle correlation can be neglected, it enables us to evaluate the cross-correlation functions from a one-particle simulation. The Monte Carlo method is proven to be a fruitful procedure to obtain the relevant correlation functions (and thus the frequency-dependent spectral density). Indeed, it enables us to solve the appropriate master equation at a kinetic level without approximations and in the presence of an electric field of arbitrary strength. The satisfactory agreement obtained with existing mesoscopic theories[15-17] (in the limit of their validity) and available experiments[29,30] fully supports the physical plausibility of the present approach and gives us confidence in predicting that this method will be further developed to account for refinements in the theory.

ACKNOWLEDGMENTS

APPENDIX A

Here we shall prove Eq. (2). The total current $\mathbf{j}(\mathbf{r},t)$ consists of two contributions, the conduction current density $\mathbf{j}_c(\mathbf{r},t)$ given by

$$\mathbf{j}_c(\mathbf{r},t)=e\sum_{i=1}^{N_I}\mathbf{v}_i^r(t)\delta(\mathbf{r}-\mathbf{r}_i(t)) \tag{A1}$$

and the displacement current density $\mathbf{j}_d(\mathbf{r},t)$ given by

$$\mathbf{j}_d(\mathbf{r},t)=\epsilon_0\epsilon_r\frac{\partial \mathbf{E}(\mathbf{r},t)}{\partial t} . \tag{A2}$$

From the continuity and the Maxwell equations follows

$$\mathrm{div}\,\mathbf{j}=\mathrm{div}(\mathbf{j}_c+\mathbf{j}_d)=0 . \tag{A3}$$

If we take the direction of the device as x the total current through a cross-sectional area A perpendicular to this direction is given by

$$I(x,t)=\int\int_A dy\,dz\,j_x(\mathbf{r},t) . \tag{A4}$$

If the length of the device is small compared to its lateral

dimensions, Eq. (A3) implies that the total current through each cross-sectional area is the same, thus $I(x,t)$ is independent of x. Then we can write

$$\begin{aligned}
I(t)&=\frac{1}{L}\int_0^L I(t)dx\\
&=\frac{1}{L}\int_0^L dx\int\int_A dy\,dz\left[e\sum_{i=1}^{N_I}v_{ix}^r(t)\delta(\mathbf{r}-\mathbf{r}_i(t))\right.\\
&\qquad\qquad\left.+\frac{\partial E_x(\mathbf{r},t)}{\partial t}\right]\\
&=\frac{e}{L}\sum_{i=1}^{N_I}v_{ix}^r(t)-\epsilon_0\epsilon_r A\frac{\partial}{\partial t}[V(L)-V(0)] .
\end{aligned} \tag{A5}$$

We have used the fact that $\mathbf{E}$ is the gradient of the potential V and the contacts at $x=0$ and $x=L$ are equipotential surfaces. If the voltage applied to the contacts is kept constant with time, then the last term in Eq. (A5) vanishes and we obtain the final result

$$I(t)=\frac{e}{L}\sum_{i=1}^{N_I}v_{ix}^r(t)=\frac{e}{L}N_I v_d^r(t)=\frac{e}{L}N(t)v_d(t) . \tag{A6}$$

APPENDIX B

Here we shall derive expression (7). Be definition we have

$$\delta I(t)=\frac{e}{L}[N(t)v_d(t)-\langle N(t)v_d(t)\rangle] . \tag{B1}$$

By linearizing Eq. (2) through $N(t)=\langle N\rangle+\delta N(t), v_d(t)=\langle v_d\rangle+\delta v_d(t)$, Eq. (B1) becomes

$$\begin{aligned}
\delta I(t)&=\frac{e}{L}[\langle N\rangle\langle v_d\rangle+\langle N\rangle\delta v_d(t)+\langle v_d\rangle\delta N(t)+\delta N(t)\delta v_d(t)-\langle N(t)v_d(t)\rangle]\\
&=\frac{e}{L}[\langle N\rangle\delta v_d(t)+\langle v_d\rangle\delta N(t)+\delta N(t)\delta v_d(t)-\langle \delta N(t)\delta v_d(t)\rangle]\\
&\simeq\frac{e}{L}[\langle N\rangle\delta v_d(t)+\langle v_d\rangle\delta N(t)]
\end{aligned} \tag{B2}$$

since the term $[\delta N(t)\delta v_d(t)-\langle \delta N(t)\delta v_d(t)\rangle]$, being of second order in fluctuations, can be neglected.

APPENDIX C

Here we shall prove Eqs. (16)–(20). According to the definition in Eq. (5), the autocorrelation function of reduced velocity fluctuations (AFRVF) can be decomposed in the diagonal and off-diagonal contributions as

$$\begin{aligned}
\langle\delta v_d^r(0)\delta v_d^r(t)\rangle&=\frac{1}{N_I^2}\sum_{i,j=1}^{N_I}\langle[v_i^r(0)-\langle v_d^r\rangle][v_j^r(t)-\langle v_d^r\rangle]\rangle\\
&=\frac{1}{N_I}\langle[v_i^r(0)-\langle v_d^r\rangle][v_i^r(t)-\langle v_d^r\rangle]\rangle+\frac{1}{N_I^2}\sum_{\substack{i,j=1\\(j\neq i)}}^{N_I}\langle[v_i^r(0)-\langle v_d^r\rangle][v_j^r(t)-\langle v_d^r\rangle]\rangle .
\end{aligned} \tag{C1}$$

The off-diagonal term in the last row of Eq. (C1) describes particle-particle correlations, thus for the case of noninteracting particles it can be neglected and Eq. (16) is obtained.

Let us consider Eq. (17) which, according to Eq. (3), can be written as

$$\langle \delta N(0)\delta N(t)\rangle = \sum_{i,j=1}^{N_I} \langle [u_i(0)-\langle u\rangle][u_j(t)-\langle u\rangle]\rangle$$

$$= N_I\langle [u_i(0)-\langle u\rangle][u_i(t)-\langle u\rangle]\rangle + \sum_{\substack{i,j=1 \\ (j\neq i)}}^{N_I} \langle [u_i(0)-\langle u\rangle][u_j(t)-\langle u\rangle]\rangle . \qquad (C2)$$

The off-diagonal term in the last row of Eq. (C2) describes the cross correlations due to particle-particle interaction, thus for the case of noninteracting particles it can be neglected and the result, Eq. (18), is obtained.

Let us consider now one of the cross terms in Eq. (11) which, by using Eq. (14), can be written as

$$\langle \delta N(0)\delta v_d(t)\rangle = \frac{1}{\langle u\rangle}\left\langle \sum_{i=1}^{N_I} [u_i(0)-\langle u\rangle]\frac{1}{N_I}\sum_{j=1}^{N_I}[v_j^r(t)-\langle v_d^r\rangle]\right\rangle$$

$$-\frac{\langle v_d^r\rangle}{N_I\langle u\rangle^2}\sum_{i,j=1}^{N_I} \langle [u_i(0)-\langle u\rangle][u_j(t)-\langle u\rangle]\rangle$$

$$= \frac{1}{\langle u\rangle}\langle [u_i(0)-\langle u\rangle][v_i^r(t)-\langle v_d^r\rangle]\rangle - \frac{\langle v_d^r\rangle}{\langle u\rangle^2}\langle [u_i(0)-\langle u\rangle][u_i(t)-\langle u\rangle]\rangle$$

$$+ \sum_{\substack{i,j=1 \\ j\neq i}}^{N_I} \left[\frac{1}{\langle u\rangle N_I}\langle [u_i(0)-\langle u\rangle][v_j^r(t)-\langle v_d^r\rangle]\rangle - \frac{\langle v_d^r\rangle}{N_I\langle u\rangle^2}\langle [u_i(0)-\langle u\rangle][u_j(t)-\langle u\rangle]\rangle\right] .$$

The off-diagonal term in the last two rows of Eq. (C3) describes particle-particle correlations, thus for the case of noninteracting particles it can be neglected. By applying the same procedure to the term $\langle \delta v_d(0)\delta N(t)\rangle$, the results of Eqs. (18) and (19) are directly obtained.

*On leave from Institut für Theoretische Physik, Universität Stuttgart, Pfaffenwaldring 57, 7000 Stuttgart 80, Federal Republic of Germany.

[1]C. Jacoboni and L. Reggiani, Rev. Mod. Phys. **55**, 645 (1983).

[2]J. Zimmerman and E. Constant, Solid State Electron. **23**, 914 (1980).

[3]C. Moglestue, in *Proceedings of the 7th International Conference on Noise in Physical Systems and 1/f Noise,* edited by M. Savelli, G. Lecoy, and J. P. Nougier (North-Holland, Amsterdam, 1983), p. 23.

[4]B. Boittiaux, E. Constant, and A. Ghis, in Ref. 3, p. 19.

[5]B. R. Nag, S. R. Ahmed, and M. Deb Roy, Appl. Phys. A **41**, 197 (1986).

[6]J. Zimmerman, A. Ghis, and B. Boittiaux, in *The Physics of Submicron Semiconductor Devices,* edited by H. Grubin, D. K. Ferry, and C. Jacoboni (Plenum, New York, 1988), p. 607.

[7]D. Junevicius and A. Reklaitis, Electron. Lett. **24**, 1307 (1988).

[8]L. Reggiani, R. Brunetti, and C. Jacoboni, in *Proceedings of the 6th International Symposium on Noise in Physical Systems,* Natl. Bur. Stand. (U.S.) Spec. Publ. No. 614, edited by P. H. E. Meijer, R. D. Mountain, and R. J Soulen (U.S. GPO, Washington, D.C., 1981), pp. 414–416.

[9]P. Lugli and L. Reggiani, in *Noise in Physical Systems and 1/f Noise,* edited by A. D'Amico and P. Mazzetti (Elsevier, Amsterdam, 1986), pp. 235–238.

[10]L. Reggiani, P. Lugli, and V. Mitin, in *Proceedings of the 9th International Conference on Noise in Physical Systems,* edited by C. M. Van Vliet (World Scientific, Singapore, 1987), pp. 105–108.

[11]L. Reggiani and L. Varani, in *Proceedings of the 10th International Conference on Noise in Physical Systems,* edited by A. Ambrózy (Akadémiai Kiadó, Budapest, 1990), pp. 95–98.

[12]P. Bordone, L. Reggiani, L. Varani, and V. Mitin, in Ref. 11,

pp. 99–102.

[13]L. Reggiani, P. Lugli, and V. Mitin, Phys. Rev. Lett. **60**, 736 (1988).

[14]L. Reggiani, P. Lugli, and V. Mitin, *Proceedings of the 19th International Conference on the Physics of Semiconductors,* edited by W. Zawadzki (Wrodawska Drukarnia Naukowa, Wroclaw, 1988), p. 1723.

[15]R. E. Burgess, Proc. Phys. Soc. London Sect. B **69**, 1020 (1956).

[16]M. Lax, Rev. Mod. Phys. **32**, 25 (1960).

[17]K. M. Van Vliet and J. R. Fasset, in *Fluctuation Phenomena in Solids,* edited by R. E. Burgess (Academic, New York, 1965), p. 267.

[18]A. Van der Ziel, *Noise, Source, Characterization, Measurement* (Prentice-Hall, New Jersey, 1970).

[19]B. Pellegrini, Phys. Rev. B **34**, 5921 (1986).

[20]K. M. Van Vliet, J. Math. Phys. (New York) **12**, 1981, 1998 (1971).

[21]P. Lugli, L. Reggiani, and J. J. Niez, Phys. Rev. B **40**, 12 382 (1989).

[22]L. Reggiani, P. Lugli, and V. Mitin, Appl. Phys. Lett. **51**, 925 (1987).

[23]L. Reggiani, L. Varani, J. C. Vaissiere, J. P. Nougier, and V. Mitin, J. Appl. Phys. **66**, 5404 (1989).

[24]L. Reggiani, R. Brunetti, and E. Normantas, J. Appl. Phys. **59**, 1212 (1986).

[25]L. Reggiani, *Hot Electron Transport in Semiconducors,* Vol. 58 of *Topics in Applied Physics* (Springer-Verlag, Berlin, 1985).

[26]L. Reggiani and V. Mitin, Rivista del Nuovo Cimento **12**, No. 11 (1989).

[27]R. Brunetti and C. Jacoboni, Phys. Rev. B **29**, 5739 (1984).

[28]P. J. Price, J. Appl. Phys. **6**, 949 (1960).

[29]D. Gasquet, B. Azais, J. C. Vaissiere, and J. P. Nougier, in

Noise in Physical Systems and 1/f Noise–1985, edited by A. D'Amico and P. Mazzetti (North-Holland, Amsterdam, 1985), p. 231.

[30]J. C. Vaissiere, Ph.D. dissertation, University of Montpellier, 1986 (unpublished).

[31]J. L. Hartke, J. Appl. Phys. **39**, 4871 (1969).

[32]M. Ieda, G. Sawa, and S. Kato, J. Appl. Phys. **42**, 3737 (1971).

[33]V. N. Abakumov, L. N. Kreshchuk, and I. N. Yassievich, Fiz. Tekh. Poluprovodn. **12**, 264 (1978) [Sov. Phys.—Semicond. **12**, 264 (1978)].